Thermochimica Acta, 155 (1989) 39–56
Elsevier Science Publishers B.V., Amsterdam – Printed in The Netherlands

EMF INVESTIGATION OF Al–Si, Al–Fe–Si AND Al–Ni–Si LIQUID ALLOYS

M. BONNET, J. ROGEZ and R. CASTANET

Centre de Thermodynamique et de Microcalorimétrie du CNRS, 26 rue du 141eme R.I.A., 13003 Marseille (France)

(Received 22 February 1989)

ABSTRACT

The partial free enthalpy of Al in liquid Al–Si, Al–Ni, Al–Fe–Si and Al–Ni–Si melts on the Al-rich side was determined by the concentration cell method:

$(-)\mathrm{Ta}\,|\,\mathrm{Al}\,|\,\mathrm{Al}^{3+}$ in LiCl–KCl eut. $|$alloy$|\,\mathrm{Ta}(+)$

The measurements were made on both heating and cooling in steps of 30 K from about 850 to about 1300 K.

The activity of Al in the four systems under investigation shows negative deviations from ideality. However, additions of Fe into Al–Si alloys reduce the deviations whereas additions of Ni increase it. Such a conclusion corresponds with the larger ability of Al–Ni–Si-based alloys to give glasses compared with Al–Fe–Si alloys as the ability of liquids to give amorphous states by rapid quenching is strongly correlated with short range order.

INTRODUCTION

Many multi-component alloys containing mainly Al, Fe, Ni and Si are promising glass-formers. It is well known that Al–Ni–Si-based alloys are better glass formers than those of Al–Fe–Si. However although the thermodynamic properties of Al–Fe–Si alloys have been measured [1], this is not the case for the Al–Ni–Si ternary. Therefore the purpose of this work was to measure the partial free enthalpy of Al in Al–Ni–Si liquids in order to compare the thermodynamic behaviour of Al–Fe–Si and Al–Ni–Si.

In order to check the electrochemical cell, the Al–Si and Al–Ni binary systems were first investigated as the partial free enthalpy of Al in these liquids has already been measured by Berthon et al. [2] and Schaefer and Gokcen [3,4] and assessed by Murray and McAlister [5] and by Dörner and al. [6].

EXPERIMENTAL

The aluminium activity in the Al–Si and Al–Ni binaries and in the Al–Fe–Si and Al–Ni–Si ternaries was investigated by concentration cells of

0040-6031/89/$03.50

the type

$(-)\mathrm{Ta}\,|\,\mathrm{Al}\,|\,\mathrm{Al}^{3+}$ in the electrolyte $|$ alloy $|\,\mathrm{Ta}(+)$

As Al^{3+} is the common ion, the EMF between the tantalum electrodes, E, can be written

$$E = -\frac{G_{Al}}{3F} = -\frac{RT}{3F} \ln a_{Al} \tag{1}$$

where G_{Al} and a_{Al} are respectively the partial free enthalpy and the activity of Al in the alloy, T is the absolute temperature and $F = 96\,847$ coulombs.

The electrochemical cell must be reversible, i.e. there is no reaction when no current is flowing. For the same reason the electric current evolved during the measurements must be as low as possible to prevent any consumption or formation of reactant. Moreover it must be ensured that the only process which generates the EMF is the reaction under consideration. There must be no reaction with the electrodes which would modify the interfaces and induce some additional EMF. All these conditions were verified during the measurements.

The partial enthalpy and entropy of Al can be deduced from the measurements of E with respect to temperature but it is obvious that the accuracy is lowered when compared to calorimetric measurements, especially at high temperature. We did not take into account the temperature dependence of E, even when linear, except in the case of Al–Si where the scattering was exceptionally low. However some phase boundaries in the alloys and the change of reference state of pure Al could be deduced from the breaks in E with respect to temperature.

The electrochemical cell

The device used in this work was very close to that which was employed in our last investigation on Al–Sn and Al–Te binary alloys [7]. As shown in Fig. 1, the electrochemical cell consisted of an alumina crucible in which ten small crucibles were placed together. The tantalum electrodes were insulated from the electrolyte with welded alumina tubes. Silica sheaths prevented the corrosion of tantalum by chloride vapours in the highest part of the cell. The crucibles lay on an alumina dish kept in place by an alumina tube cemented on the main central tube which contained the thermocouple used for the temperature determination. This device was immersed in the liquid electrolyte and placed in the minimum temperature-gradient area of the furnace. The cell was closed by a stainless steel cover crossed over by the electrode wires.

The tightness of the cell was ensured by epoxy resin and a water-cooled "viton" torus. The device was under pure argon atmosphere. The main

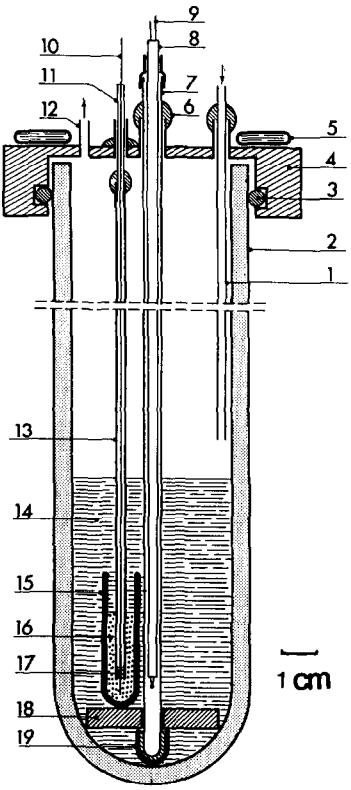

Fig. 1. The electrochemical cell: 1, inert gas input (argon); 2, alumina tube $\Phi_e = 55$ mm, $\Phi_i = 47$ mm, $h = 450$ mm; 3, gas-tightness sealed with "viton" torus; 4, stainless steel cover; 5, water cooling; 6, gas-tightness sealed with epoxy resin; 7, alumina tube, one end closed; 8, alumina tube, two holes; 9, thermocouple Pt/Pt–10 mass% Rh for temperature measurement; 10, tantalum electrode, $\Phi = 0.5$ mm; 11, silica insulating of the electrodes; 12, inert gas output (argon); 13, alumina insulating of the electrodes, $\Phi_e = 3$ mm $\Phi_i = 1.5$ mm, $h = 400$ mm; 14, electrolyte; 15, alumina crucible, $\Phi_e = 10$ mm $\Phi_i = 7$ mm, $h = 38$ mm; 16, alloy (0.4 cm^3 $h \approx 20$ mm); 17, alumina welding over the electrode; 18, alumina dish supporting the crucibles; 19, alumina tube cemented on tube 7.

alumina tube was placed in a stainless steel tube in order to homogenize the temperature and to act as an electrical shield.

The maximum temperature of the furnace was 1523 K and the temperature measurement was performed with a Pt/Pt–10 mass% Rh thermocouple previously calibrated at ± 2 K. The temperature of the cell was controlled at ± 1 K. Because alumina shows a non-negligible electrical conduction at high temperature, the power supply of the furnace was isolated to avoid any perturbation of the EMF to be measured. The EMF was measured with an electrometer with an input impedance of 2×10^{14} Ω and an accuracy of ± 10 μV (Keithley instrument). The current through the cell was always less than 10^{-16} A. A multipole switch with silver grains was inserted in the EMF measurement circuit.

Electrolyte

The electrolyte has to be selected according to the following criteria: the constituents must have closely related ionic conductivities; the electrolyte must be completely ionized; and its vapour pressure must be low at high temperature. For these reasons, solid electrolytes are useful beyond 1300 K but good solid–solid contacts are difficult to obtain and these interfaces may involve large uncertainties in the measurements. The alkaline halogenides are generally used in spite of their great tendency for hygroscopy. Their ionic conductivity is high.

For such investigations, pure NaCl [8] or a mixture of NaCl and KCl (melting point of the eutectic, 918 K) [3,4,10] have been used. The partial pressure above the melt is about 10 Torr. Like Massart et al. [9], we used the LiCl–KCl eutectic as the solvent for $AlCl_3$, the sublimation temperature of which is 451 K under one atmosphere. However, the introduction of $AlCl_3$ into the melt without losses was not easy. Moreover it must be noted that too large a concentration of aluminium chloride in the melt may drastically increase the corrosion effects. Schaefer and Gokcen [3,4], Wilder and Elliott [10] and Hillert [8] prepared the electrolyte separately in a quartz tube. The mixture was introduced into the tube and then heated up to the melting point of the lowest melting constituent. After cooling, the solid or liquid mixture was placed in the cell.

In this work, the LiCl–KCl eutectic was prepared directly in the electrochemical cell. The melting point of this eutectic (42 mol% KCl) is 623 K. The powders corresponding to 3.22 mol of the eutectic were dried under vacuum at 600 K for 12 h and kept under argon static pressure in order to prevent the sublimation of LiCl. The solid mixture was then melted at 920 K over 30 min (heating rate 150 K min^{-1}) and then cooled slowly to 673 K. A good homogeneity can be obtained by keeping the electrolyte at this temperature for 1 h. Pellets of $AlCl_3$ (45 mmol) were then quickly introduced into the liquid which was kept at 773 K for 2 h. The chemical materials were purchased from Fluka (puriss p.a. quality). In a preliminary experiment, the electrolyte was prepared in this way in a quartz tube. The liquid obtained was perfectly clear without sediment. No condensation was observed on the walls of the tube. The dissolution of the different components was complete.

Electrodes

The electrodes must be chemically compatible with the electrolyte and the alloys investigated. Among the different possible materials which were considered (Ta, W, Mo), tantalum is the most resistant towards corrosion effects. The works of Wilder and Elliott [10] at 1173 K, Massart et al. [9] and Perakis and Desré [1] at 1273 K have shown that Al_3Ta is produced at the

interface between the alloy and the electrode. This compound acts as a chemical shield for pure tantalum. In contrast, molybdenum and tungsten aluminides lead to brittleness of the electrodes. Tantalum was used up to 1923 K by Lawthers and Sama [11] in a liquid electrolyte after Al_3Ta was layered by sputtering of an Al–Sn alloy. Pure tantalum (3N5) was purchased from Ballofet. A gas-tight welding was made between the electrode and the insulating alumina tube. The length of the tube was 400 mm and its diameter was 1.6 mm. The diameter of the metallic electrode was 0.5 mm and its uninsulated part was 5 mm long.

Alloy synthesis and the building of the electrochemical cell

The alloys were prepared in alumina crucibles of 38 mm height. Ten crucibles were placed together in the cell (seven alloys and three pure aluminium references). Each crucible contained about 25 mmol of metal. The purity of the aluminium sheets (0.5 mm thickness) and silicon pieces (Ventron products) were 4 N and 6 N respectively.

The electrodes must be carefully introduced into the samples without any contact with the electrolyte. No oxidation must occur at this stage. Introducing the tantalum electrodes directly into the metallic melt is not suitable because the alumina present on the aluminium surface disturbs the electrode–alloy junctions. There must be no gas flow because the subsequent aluminium losses introduce non-negligible variations in the composition of the samples. For these reasons we chose to prepare the alloy and to introduce the electrodes into them at the same stage. The crucibles containing the weighed elements were placed in a quartz tube with the electrode at the bottom of the crucible. The pure aluminium or alloys were then heated under vacuum a few degrees above their melting point. Then the samples with their electrodes were introduced into the main alumina tube containing the electrolyte at 773 K. The cell was then heated at 1253 K with a heating rate of about 100 K h^{-1} in order to homogenize the alloys and to mechanically stabilize the electrodes in the different melts. In order to improve the reproducibility of the EMF, it was necessary, typically, to keep the cell for 12 h at the highest temperature of measurement (about 1023 K).

RESULTS

The EMF between the alloys and the three reference electrodes (pure Al) was measured on heating and on cooling (six measurements for each alloy at each temperature) every 30 K. This meant that the reversibility of the cell could be re-checked. The EMF measurements were carried out after 1 h on heating and 1.5 h on cooling at any given temperature. The scatter of the data is larger at high temperatures ($T > 1073$ K) where electrical perturba-

tions occur, and with solid Al ($T < 933$ K) as reference, due to less efficient ionic diffusion. The temperature was determined from the EMF of a Pt/Pt–10%Rh thermocouple at ± 2 K. The composition of the alloys investigated was controlled by chemical analysis (± 0.5 at.%).

Binary alloys

Seven Al–Si alloys ($0.65 < x_{Al} < 1$) and three Al–Ni alloys ($0.84 < x_{Al} < 1$) were investigated from 859 to 1259 K (Al–Si) and from 873 to 1233 K (Al–Ni). The results are shown in Fig. 2 (Al–Si) and Fig. 3 (Al–Ni). As an example, the EMF data are given in Table 1 for Al–Si ($x_{Al} = 0.021$).

When the solidification temperature of the alloy under investigation is less than the melting point of Al (933 K), the curve $E = f(T)$ can be divided into three straight lines, i.e. E undergoes two breaks corresponding to the melting of pure Al (low temperature break) and to the liquidus temperature (high temperature break). The slope difference at 933 K corresponds to the enthalpy of melting of Al

$$H^{fus}(Al) = 3FT^{fus}\left[\frac{dE}{dT_s} - \frac{dE}{dT_l}\right] \quad (2)$$

This yields $H^{fus}(Al) = 10 \pm 1$ kJ mol^{-1} instead of 10.8 kJ mol^{-1}, according to Hultgren et al. [12].

The liquidus temperatures of Al–Si and Al–Ni alloys determined from the high temperature breaks of $E = f(T)$ lead to the phase diagrams shown in Figs. 4 and 5, in good agreement with Hansen and Anderko [13].

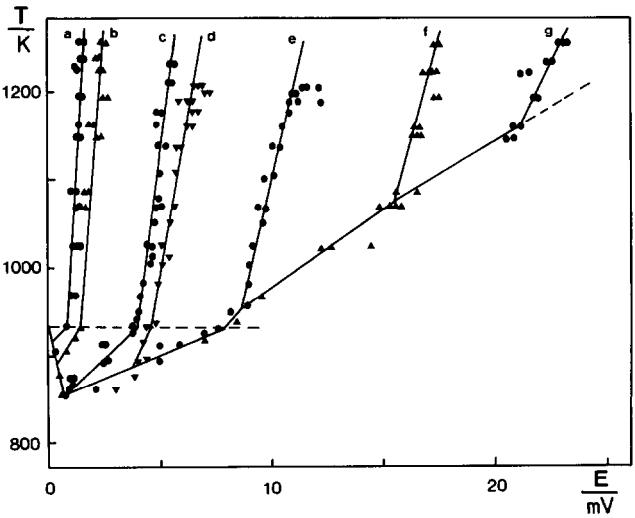

Fig. 2. EMF of Al/Al–Si cells with respect to temperature for different mole fractions of Al: x_{Al}, 0.979 (a); 0.950 (b); 0.892 (c); 0.850 (d); 0.801 (e); 0.699 (f); and 0.650 (g).

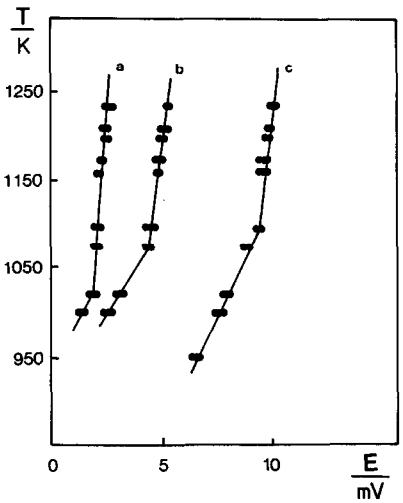

Fig. 3. EMF of Al/Al–Ni cells with respect to temperature for different mole fractions of Al: x_{Al}, 0.9516 (a); 0.9054 (b); and 0.8496 (c).

The EMF data were fitted according to a linear dependence on T

$$E = a + bT \tag{3}$$

The coefficients obtained are given in Tables 2 and 3 (column 2) with the partial free enthalpy of Al. The correlation coefficients were typically about

TABLE 1

EMF between pure Al and $Al_{0.079}Si_{0.021}$

T (K)	E (mV)			E (mV)
	E_1	E_2	E_3	
Ref. Al(l)				
1253	1.12	1.08	1.15	1.12
1242	1.10	0.85	1.15	1.03
1226	0.85	0.94	1.03	0.94
1197	1.10	1.21	1.16	1.16
1158	1.12	1.18	1.50	1.15
1151	1.02	1.10	1.18	1.10
1088	0.80	0.76	0.92	0.83
1070	1.00	0.99	1.11	1.03
1024	0.90	0.86		0.88
969	0.88	0.80		0.84
933	0.75	0.70		0.73
Ref. Al(s)				
923	0.35	0.30		0.33
900	0.25	0.30		0.28
853	0.50	0.42		0.46

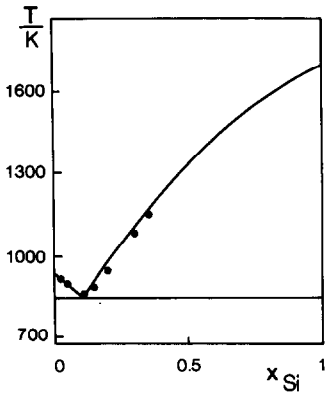

Fig. 4. Phase diagram of the Al–Si binary system according to ref. 13 (solid lines) and this work (points).

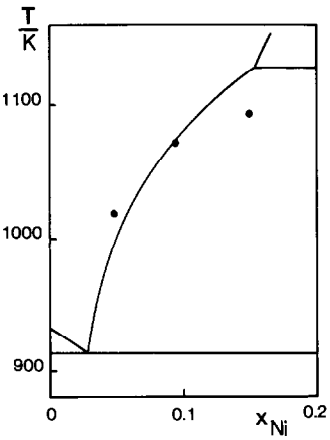

Fig. 5. Phase diagram of the Al–Ni binary system on the Al-rich side according to ref. 13. The three points correspond to the breaks in $E = f(T)$ (see Fig. 3).

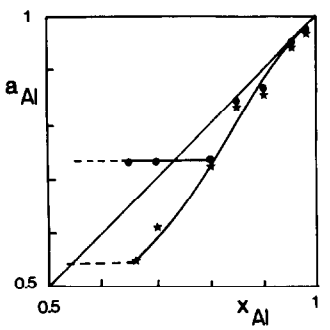

Fig. 6. Activity of aluminium in binary Al–Si melts with respect to the mole fraction of Al at 953 (●) and 1160 K (★).

TABLE 2

Thermodynamic functions of formation at 1160 K of liquid Al–Si binary alloys referred to pure liquid aluminium and silicon

x_{Al}	E (mv) $= f(T)$	a_{Al}	γ_{Al}	G_{Al} (kJ mol^{-1})	H_{Al} (kJ mol^{-1})	S_{Al} (J mol^{-1} K^{-1})	G^{xs} (kJ mol^{-1})	G^{xs}_{Al} (kJ mol^{-1})	T_L (K)
0.979	$E = 0.00097T - 0.10217$	0.9698	0.9906	−0.296	0.029	0.281	−1.956	−0.091	918
0.950	$E = 0.00309T - 1.7838$	0.9482	0.9981	−0.513	0.516	0.894	−1.956	−0.018	893
0.892	$E = 0.00468T - 0.59019$	0.8648	0.9695	−1.401	0.171	1.355	−3.744	−0.299	853
0.850	$E = 0.00648T - 1.66025$	0.8388	0.9868	−1.695	0.481	1.876	−5.408	−0.128	888
0.801	$E = 0.00946T - 0.618$	0.7328	0.9148	−2.997	0.179	2.738	−6.980	−0.857	953
0.699	$E = 0.00976T + 4.814$	0.6161	0.8814	−4.671	−1.393	2.825	−9.924	−1.217	1076
0.650	$E = 0.02197T - 5.110$	0.5425	0.8346	−5.898	1.479	6.359	−11.301	−1.743	1161

TABLE 3

Thermodynamic functions of aluminium at 1173 K in liquid Al–Ni binary alloys referred to pure liquid aluminium

x_{Al}	E (mV) $= f(T)$	G_{Al} (kJ mol^{-1})	G_{Al}^{xs} (kJ mol^{-1})
0.9516	$0.00261T - 0.83984$	−0.149	−0.63
0.9054	$0.00570T - 1.90188$	−0.416	−1.39
0.8496	$0.00525T + 3.48443$	−1.203	−2.79

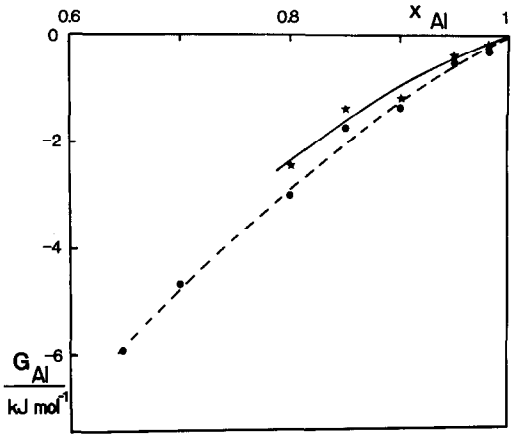

Fig. 7. Partial molar free enthalpy of Al in binary Al–Si melts with respect to the mole fraction of Al at 953 (★) and 1160 K (●).

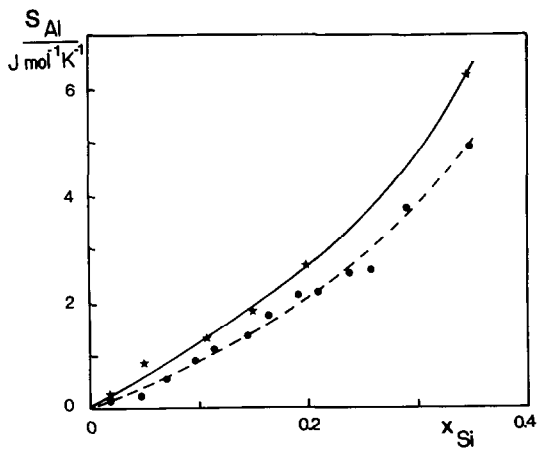

Fig. 8. Partial molar entropy of Al in binary Al–Si melts with respect to the mole fraction of Al according to ref. 3 (●) and this work (★).

0.9 for liquid alloys. The activity of Al in Al–Si liquid alloys is shown at 953 and 1160 K in Fig. 6. The partial free enthalpy of Al, G_{Al}, and the partial entropy of Al, S_{Al}, at 1160 K are shown respectively in Figs. 7 and 8. The agreement between our results and those of Murray and McAlister [5] and those of Schaefer and Gokcen [3,4] is good. By integrating the Gibbs–Duhem relation, the integral free enthalpy of formation of the liquid Al–Si alloys were calculated and we found for example $G_{Al}(Al–Si) = -9.8$ kJ mol^{-1} at $x_{Al} = 0.7$ and $T = 1160$ K instead of -10.9, according to Murray et al. [5]. Our results for S_{Al} agree well with those of Berthon et al. [2] as shown in Fig. 8. We found $G_{Al}(Al–Ni) = -0.63$ kJ mol^{-1} at $x_{Al} = -0.95$ and $T =$ 1173 K, instead of -0.59 according to Schaefer and Gokcen whose results are somewhat scattered [3,4].

Ternary alloys

In order to check the electrochemical cell again in the case of ternary Al-based alloys, we investigated five Al–Fe–Si alloys with the same ratio $\rho = x_{Fe}/x_{Si} = 0.501$. The thermodynamic data obtained are given in Table 4 with the liquidus temperatures deduced from the breaks in E with respect to T. The activity of Al in ternary liquid alloys is plotted in Fig. 9 at 1173 K.

TABLE 4

Thermodynamic functions of aluminium at 1173 K in liquid Al–Fe–Si ($\rho = 0.501$) ternary alloys referred to pure liquid aluminium

Composition	E (mV) $= f(T)$	a_{Al}	γ_{Al}	G_{Al} (kJ mol^{-1})	G_{Al}^{xs} (kJ mol^{-1})	T_L [a] (K)
$x_{Al} = 0.895$ $x_{Fe} = 0.036$ $x_{Si} = 0.069$	$E = 0.00242T + 0.98920$	0.8926	0.9973	−1.108	−0.026	1026
$x_{Al} = 0.794$ $x_{Fe} = 0.069$ $x_{Si} = 0.136$	$E = 0.00502T + 2.60861$	0.7770	0.9787	−2.460	−0.210	1048
$x_{Al} = 0.744$ $x_{Fe} = 0.087$ $x_{Si} = 0.169$	$E = 0.01180T - 2.74403$	0.7195	0.9670	−3.211	−0.327	1073
$x_{Al} = 0.702$ $x_{Fe} = 0.100$ $x_{Si} = 0.198$	$E = 0.01100T - 0.27690$	0.6875	0.9793	−3.655	−0.204	1093
$x_{Al} = 0.645$ $x_{Fe} = 0.118$ $x_{Si} = 0.237$	$E = 0.00993T + 3.63200$	0.6354	0.9851	−4.423	−0.147	1109

[a] T_L, liquidus temperature.

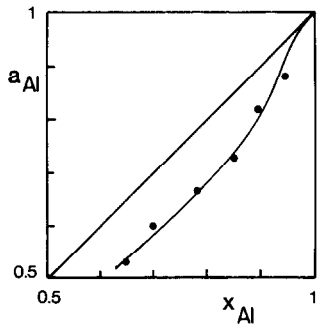

Fig. 9. Activity of Al in ternary Al–Ni–Si melts at 1173 K for $\rho = x_{Ni}/x_{Si} = 0.215$ with respect to mole fraction of Al.

The partial molar free enthalpy of Al at 1173 K is shown in Fig. 10 with the results of Perakis and Desré [1] at the same temperature and the x_{Fe}/x_{Si} ratio. As can be seen, the agreement is very good.

The compositions of the ternary Al–Ni–Si alloys investigated lie mainly along three lines with $\rho = x_{Ni}/x_{Si} = 0.066$, 0.215 and 1.020. In order to study the effect of substitution of Si by Ni at high Al content, we also measured the partial free enthalpy of Al in three ternary alloys at $x_{Al} = 0.85$ ($\rho = 0.282$, 0.492 and 0.771). As an example, the EMF against T for $\rho = 0.215$ is given in Table 5 and shown in Fig. 11. The activity of Al at 1173 K for $\rho = 0.215$ is plotted against x_{Al} on Fig. 9 and the thermodynamic data calculated are given in Tables 6–9 with the liquidus temperatures.

The partial molar free enthalpy of Al is plotted with respect to composition in Fig. 12. It shows that G_{Al} increases when ρ increases at high Al

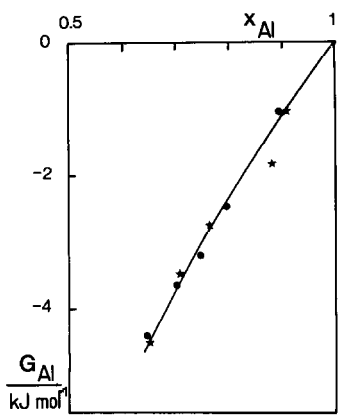

Fig. 10. Partial molar free enthalpy of Al in ternary Al–Fe–Si melts ($x_{Fe}/x_{Si} = 0.501$) at 1173 K according to Perakis and Desré [1] (★) and this work (●) with respect to mole fraction of Al.

TABLE 5

EMF between pure liquid Al and $Al_{0.7789}Si_{0.1702}Ni_{0.0511}$ ($\rho = 0.215$)

T (K)	E (mV)			E (mV)
	E_1	E_2	E_3	
1257	14.70	14.50	13.91	14.37
1243	14.30	14.10	14.47	14.29
1221	14.15	13.98	14.31	14.15
1200	13.97	14.12	13.85	13.98
1186	13.80	13.77	13.91	13.83
1173	13.71	13.65	13.84	13.73
1149	13.63	13.54	13.48	13.55
1136	13.45	13.61	13.39	13.48
1127	13.41	13.28	13.31	13.33
1100	13.21	13.12		13.17
1086	13.10	13.06	13.21	13.12
1058	12.93	12.84	12.77	12.85
1028	12.20	12.41	12.16	12.26
1000	10.30	10.12	10.41	10.28
973	7.98	8.31	8.45	8.25
968	6.81	6.73	6.96	6.83
948	5.80	6.01	5.74	5.85

TABLE 6

Thermodynamic functions of aluminium at 1173 K in liquid Al–Ni–Si ($\rho = 0.066$) ternary alloys referred to pure liquid aluminium

Composition	E (mV) = $f(T)$	a_{Al}	γ_{Al}	G_{Al} (kJ mol^{-1})	G_{Al}^{xs} (kJ mol^{-1})	T_L [a] (K)
$x_{Al} = 0.9423$ $x_{Si} = 0.0531$ $x_{Ni} = 0.0046$	$E = 0.00608T - 2.36675$	0.8681	0.9213	−1.379	−0.800	
$x_{Al} = 0.9102$ $x_{Si} = 0.1060$ $x_{Ni} = 0.0070$	$E = 0.00975T - 3.12554$	0.7814	0.8585	−2.406	−1.488	866
$x_{Al} = 0.8461$ $x_{Si} = 0.1430$ $x_{Ni} = 0.0109$	$E = 0.01009T - 0.16975$	0.7073	0.8360	−3.377	−1.747	908
$x_{Al} = 0.7990$ $x_{Si} = 0.1892$ $x_{Ni} = 0.0119$	$E = 0.01162T - 0.68924$	0.6538	0.8182	−4.145	−1.957	958
$x_{Al} = 0.7030$ $x_{Si} = 0.2820$ $x_{Ni} = 0.0147$	$E = 0.02292T - 8.56511$	0.5438	0.7735	−5.303	−1.866	1071
$x_{Al} = 0.6050$ $x_{Si} = 0.3705$ $x_{Ni} = 0.0241$	$E = 0.04171T - 27.68687$	0.5324	0.8800	−6.148	−1.247	1196

[a] T_L, liquidus temperature.

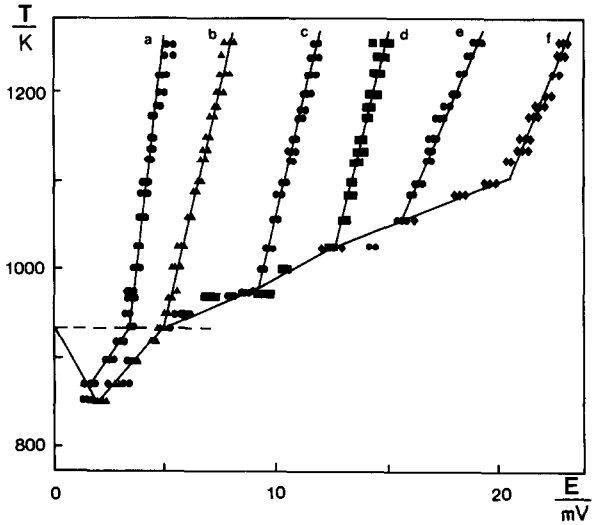

Fig. 11. EMF of Al/Al–Ni–Si cells with respect to temperature for $\rho = x_{Ni}/x_{Si} = 0.215$ and different mole fractions of Al: x_{Al}, 0.9469 (a); 0.8966 (b); 0.8493 (c); 0.7789 (d); 0.7010 (e); 0.6476 (f).

TABLE 7

Thermodynamic functions of aluminium at 1173 K in liquid Al–Ni–Si ($\rho = 0.215$) ternary alloys referred to pure liquid aluminium

Composition	E (mV) $= f(T)$	a_{Al}	γ_{Al}	G_{Al} (kJ mol^{-1})	G_{Al}^{xs} (kJ mol^{-1})	T_L [a] (K)
$x_{Al} = 0.9469$ $x_{Si} = 0.0416$ $x_{Ni} = 0.0116$	$E = 0.00462T - 1.11608$	0.8801	0.9295	−1.246	−0.713	863
$x_{Al} = 0.8966$ $x_{Si} = 0.0654$ $x_{Ni} = 0.0184$	$E = 0.00827T - 2.90211$	0.8173	0.9115	−1.968	−0.903	846
$x_{Al} = 0.8493$ $x_{Si} = 0.1230$ $x_{Ni} = 0.0276$	$E = 0.00963T - 0.56122$	0.7272	0.8562	−3.107	−1.514	978
$x_{Al} = 0.7789$ $x_{Si} = 0.1702$ $x_{Ni} = 0.0511$	$E = 0.00771T + 4.70710$	0.6649	0.8536	−3.980	−1.543	1031
$x_{Al} = 0.7010$ $x_{Si} = 0.2461$ $x_{Ni} = 0.0529$	$E = 0.01592T - 1.38675$	0.5986	0.8540	−5.004	−1.539	1058
$x_{Al} = 0.6476$ $x_{Si} = 0.2894$ $x_{Ni} = 0.0630$	$E = 0.01707T + 1.31184$	0.5309	0.8197	−6.176	−1.938	1108

[a] T_L: liquidus temperature.

TABLE 8

Thermodynamic functions of aluminium at 1173 K in liquid Al–Ni–Si ($\rho = 1.020$) ternary alloys referred to pure liquid aluminium

Composition	E (mV) $= f(T)$	a_{Al}	γ_{Al}	G_{Al} (kJ mol^{-1})	G_{Al}^{xs} (kJ mol^{-1})	T_L [a] (K)
$x_{Al} = 0.9493$, $x_{Si} = 0.0255$, $x_{Ni} = 0.2520$	$E = 0.00698T - 3.48130$	0.8696	0.9161	−1.362	−0.855	888
$x_{Al} = 0.8972$, $x_{Si} = 0.0503$, $x_{Ni} = 0.0525$	$E = 0.00737T - 2.71586$	0.8386	0.9347	−1.716	−0.658	875
$x_{Al} = 0.8016$, $x_{Si} = 0.0979$, $x_{Ni} = 0.1005$	$E = 0.00755T + 2.14533$	0.7214	0.9000	−3.184	−1.028	1000
$x_{Al} = 0.7482$, $x_{Si} = 0.1235$, $x_{Ni} = 0.1283$	$E = 0.00299T + 12.48913$	0.6220	0.8313	−4.630	−1.801	1053
$x_{Al} = 0.6939$, $x_{Si} = 0.1528$, $x_{Ni} = 0.1533$	$E = 0.00395T + 15.56051$	0.5492	0.7914	−5.845	−2.282	1130
$x_{Al} = 0.6524$, $x_{Si} = 0.1715$, $x_{Ni} = 0.1761$	$E = 0.00578T + 15.59895$	0.5147	0.7889	−6.478	−2.313	1178
$x_{Al} = 0.6001$, $x_{Si} = 0.1971$, $x_{Ni} = 0.2028$	$E = 0.00410T + 19.93846$	0.4797	0.7994	−7.164	−2.184	1225

[a] T_L:liquidus temperature.

TABLE 9

Thermodynamic functions of aluminium at 1173 K in liquid Al–Ni–Si ternary alloys ($x_{Al} = 0.85$) referred to pure liquid aluminium

Composition	E (mV) $= f(T)$	G_{Al}^{xs} (kJ mol^{-1})
$x_{Al} = 0.8479$, $x_{Si} = 0.1186$, $x_{Ni} = 0.0335$	$E = 0.00565T + 4.57249$	−1.633
$x_{Al} = 0.8423$, $x_{Si} = 0.1056$, $x_{Ni} = 0.0520$	$E = 0.00484T + 5.03100$	−1.426
$x_{Al} = 0.8440$, $x_{Si} = 0.0881$, $x_{Ni} = 0.0679$	$E = 0.00498T + 3.72367$	−1.115

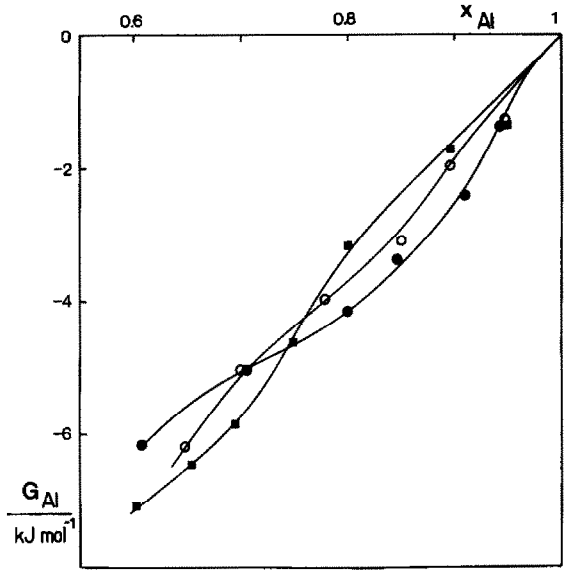

Fig. 12. Partial molar free enthalpy of Al in Al–Ni–Si melts at 1173 K with respect to mole fraction of Al and $\rho = 0.066$ (●), 0.215 (○) and 1.020 (■).

content ($x_{Al} > 0.75$) and, in contrast, decreases when ρ increases at low Al content.

DISCUSSION

The activity of Al at 1173 K is plotted against composition in Fig. 13 for Al–Si, Al–Fe–Si ($x_{Fe}/x_{Si} = 0.066$) and Al–Ni–Si ($x_{Ni}/x_{Si} = 0.066$). In all cases, a_{Al} shows negative deviations from ideality but additions of Fe or Ni into Al–Si have opposite effects because deviations are lowered by Fe and reinforced by Ni. This behaviour is in accordance with the negative interactions between Al and Ni atoms being stronger than those between Al and Fe atoms. Such a conclusion agrees well with the work of Vachet et al. [14] on the Al–Ni and Al–Si binaries. Moreover, according to Pasturel et al. [15] the interactions at high temperature between Fe and Si are lower than those between Ni and Si. The weak negative interaction between Al and Fe was pointed out by Perakis and Desré [1] who showed that it decreases with increasing Fe content.

The partial excess free enthalpy of Al is shown in Fig. 14 for $Al_{0.85}Ni_{0.15-x}Si_x$. The curve was constructed from our results on Al–Si and Al–Ni binaries, from the values interpolated at $x_{Al} = 0.85$ for $\rho = 0.066$,

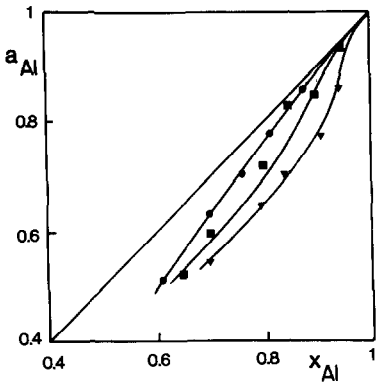

Fig. 13. Activity of Al at 1173 K in Al–Si binary melts (■), Al–Fe–Si ternary melts (●, $\rho = x_{Fe}/x_{Si} = 0.066$) and Al–Ni–Si ternary melts (▼, $\rho = x_{Ni}/x_{Si} = 0.066$) with respect to mole fraction of Al.

0.215 and 1.020, and from the three supplementary alloys prepared for this purpose. We also included the results of Schaefer and Gokcen [3,4] at 1173 K for the limiting compositions.

The dependence on composition is undoubtedly a S-shaped curve whatever we choose as limiting values, ours or those of Schaeffer and Gokcen. The minimum of G^{xs} is very close to $Al_{0.85}Si_{0.15}$ showing a marked decrease when the first Ni atoms are substituted for Si atoms. No chemical interpretation can be made concerning such a composition dependence as this requires the entropic contribution to G^{xs}.

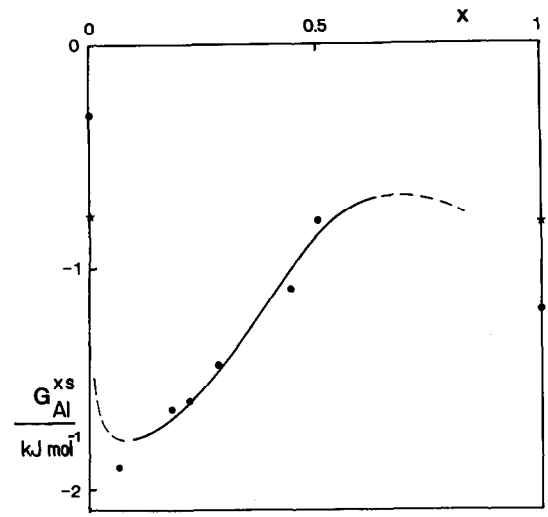

Fig. 14. Partial molar excess free enthalpy of Al at 1173 K in the $Al_{0.85}Ni_{0.15-x}Si_x$ melts with respect to x: ●, this work; ★, from Schaefer and Gokcen (3,4).

CONCLUSION

The results obtained in this work allowed us to compare the activity of Al in the Al–Si binary and in the Al–Fe–Si and Al–Ni–Si ternary systems. We can conclude that for high Al content, when Ni or Fe is added to Al–Si, the activity of Al is decreased or increased respectively. Such a conclusion is in accordance with the larger ability of Al–Ni–Si-based alloys than Al–Fe–Si-based alloys to give an amorphous state by splat-cooling from the liquid because the ability of liquids to give glasses is strongly correlated with short range order.

We observed a peculiar S-shaped composition dependence of the excess partial free enthalpy of Al for ternary $Al_{0.85}Ni_{0.15-x}Si_x$ liquid alloys. This dependence could not be explained in the context of this work as further calorimetric measurements are required in order to deduce the partial entropy of Al.

REFERENCES

1 J. Perakis and P. Desré, Rev. Int. Hautes Temp. Refract., 10 (1973) 79.
2 O. Berthon, G. Petot-Ervas, C. Petot and P. Desré, C.R. Acad. Sci. Paris, 268C (1969) 1939.
3 S.C. Schaefer and N.A. Gokcen, High Temp. Sci., 11 (1979) 31.
4 S.C. Schaefer, Int. Rep., 7896 (1974) and 7993 (1975), Natl. Bureau of Mines, U.S.A.
5 J.L. Murray and A.F. McAlister, Bull. Alloy Phase Diagram, 5(1) (1984) 74.
6 P. Dörner, E.Th. Henig, H. Krieg, H.L. Lukas and G. Petzow, Calphad 4(4) (1980) 241.
7 J. Blot, J. Rogez and R. Castanet, J. Less-Common Met., 118 (1986) 67.
8 M. Hillert, Thesis, Massachussets Inst. Techn., MA, U.S.A., 1954.
9 G. Massart, F. Durand and E. Bonnier, Bull. Soc. Chim. Fr., 15 (1965) 87.
10 T.C. Wilder and J.F. Elliott, J. Electrochem. Soc., 107(7) (1960) 628 and 111(3) (1964) 352.
11 M. Lawthers and H. Sama, Met. Soc. Conf., 18 (1961) 819.
12 R. Hultgren, P.D. Desai, D.T. Hawkins, M. Gleiser, K.K. Kelley and D.D. Wagman, Selected Values of Thermodynamic Properties of the Elements, American Society of Metals, Metals Park, OH, 1973.
13 H. Hansen and K. Anderko, Constitution of Binary Alloys, McGraw Hill, New York, 1958.
14 F. Vachet, P. Desré and E. Bonnier, C.R. Acad. Sci. Paris, 260C (1965) 453.
15 A. Pasturel, P. Hicter and F. Cyrot-Lackmann, J. Less-Common Met., 92(1) (1983) 105.